Physica Medica 65 (2019) 191–199

Contents lists available at ScienceDirect

Physica Medica

journal homepage: www.elsevier.com/locate/ejmp

Original paper

Effect of dose rate in hypofractionated radiotherapy

V.Y. Kuperman*

Medical Physics Support, Inc., 7110 Pelican Island Dr., Tampa, FL 33634, USA

ARTICLE INFO

Keywords:
Biologically effective dose
Hypofractionation
Dose rate
Radiation protraction

ABSTRACT

Purpose: To evaluate how dose rate affects radiobiological properties of hypofractionated radiotherapy.
Methods: This study is based on the linear-quadratic (LQ) model used to determine biologically effective dose (BED). Changes in the biologically effective dose in normal tissue (BED_{nt}) are studied as a function of number of fractions and dose rate under the condition of fixed BED in the treatment target (BED_{tar}).
Results: In this study we demonstrate that compared to standard fractionation, hypofractionation can either decrease or increase BED_{nt} depending on the average dose rate. In the considered examples, maximum value of BED_{nt} in the spinal cord varies monotonically with number of fractions (N_f) when dose rate is sufficiently high so that the corresponding fraction time is much smaller than characteristic repair half-lives for malignant and normal cells. In contrast, in the case of a lower dose rate of 300 MU/min, BED_{nt} in the cord can vary non-monotonically with N_f. In the later case, there exists optimum number of fractions which corresponds to the minimum BED_{nt}. It is shown that in the case when radiation induced sublethal damage is repaired faster in the target than in the affected organ at risk (OAR), increasing dose rate helps lower BED_{nt}.
Conclusion: We have demonstrated that, as compared to standard fractionation, hypofractionation can either increase or decrease BED_{nt} in the OAR depending on the utilized dose rate. Consequently, radiobiological assessment of hypofractionation should take into account dose rate as well as repair rates in the target and OAR.

1. Introduction

Radiobiological comparison of hypofractionation and standard fractionation has recently been studied by several investigators [1–5]. The obtained results indicate that under certain conditions, decreasing number of fractions can reduce BED_{nt} in the affected OAR if BED_{tar} in the treatment target is fixed [1–3]. Specifically, suppose that malignant cells in the target and normal cells in the OAR are characterized by the alpha/beta ratios $(\alpha/\beta)_{tar}$ and $(\alpha/\beta)_{nt}$, respectively. In several studies [1–3], it was theoretically shown that for a given target dose D_{tar} and maximum dose $D_{\max,nt}$ in the affected, serial organ at risk (e.g., spinal cord), BED_{nt} decreases with decreasing number of fractions if and only if $\frac{D_{\max,nt}}{D_{tar}} < \frac{(\alpha/\beta)_{nt}}{(\alpha/\beta)_{tar}}$. The latter conclusion is important because it establishes radiobiological rationale for hypofractionation in radiotherapy. To compare standard and hypofractionated regimen in the above mentioned studies, the linear-quadratic (LQ) model was used; however, the effect of fraction time (T) on BED wasn't considered. In contrast, in a recent study [4], it was shown that depending on the fraction time T (which is understood as the time interval between the beginning and end of therapeutic radiation during the same treatment) and for the same dose distribution, hypofractionation can either reduce or increase BED_{nt} as compared to that achieved with either standard fractionation or hyperfractionation. In the current study we focus on the effect of dose rate on the radiobiological comparison of hypofractionation and standard fractionation. In the discussion below our main assumption is that radiotherapy is delivered by using conformal or volumetric arcs for which the associated fraction time is primarily defined by dose per fraction and dose rate (see details in Section 2). Note that in [4] a different case of multiple non-coplanar beams delivered with fixed gantry angles was considered. In the latter case, fraction time is primarily defined by the duration of couch rotation between beams and is only weakly dependent on dose rate.

The objective of this work is to study how number of fractions affects BED_{nt} for different dose rates under the condition of fixed BED_{tar}. Both BED_{nt} and BED_{tar} are defined in the framework of the LQ model. We chose the LQ model for two reasons: (a) this model is normally employed to investigate different fractionation schemes, (b) LQ model can be extended to incorporate the effect of dose rate on biologically effective dose.

In the following discussion (see Sections II and III), it is demonstrated that depending on dose rate, hypofractionation can either reduce or increase BED_{nt} as compared to standard fractionation with dose per fraction of approximately 2 Gy. The obtained results can be used to

* Address: Medical Physics Support, Inc., 7110 Pelican Island Dr., Tampa, FL 33634, USA.
E-mail address: vadimkuperman@yahoo.com.

https://doi.org/10.1016/j.ejmp.2019.07.005
Received 21 March 2019; Received in revised form 4 June 2019; Accepted 9 July 2019
Available online 06 September 2019

compare different fractionation schemes for stereotactic radiosurgery (SRS) and stereotactic body radiation therapy (SBRT).

2. Methods

2.1. Protraction factors for the target and OAR

The quantity known as the biologically effective dose, is defined as the equivalent total dose required to give the same log cell kill as the schedule being studied, at an infinitely low dose-rate or with infinitely small fractions well spaced out [6,7]. In the discussion below, we assume that the considered course of radiotherapy includes N_f fractions with fraction time T, dose rate $R(t)$, dose per fraction d and total dose $D = N_f d$. In this case, BED is

$$BED = D\left(1 + \frac{Gd}{\alpha/\beta}\right), \tag{1}$$

where $d = \int_0^T R(t)dt$, α and β are the radio-sensitivities and G is known as the Lea-Catcheside protraction factor [8–10]

$$G = \frac{2}{d^2}\int_0^T R(t)\left(\int_0^t R(t')\exp(-\mu(t-t'))dt'\right)dt, \tag{2}$$

where t' is a dummy variable varying between zero and t. Note that parameter μ in Eq. (2) is referred to as the rate of repair and is defined by the repair half-life $T_{1/2}$: $\mu = \frac{\ln 2}{T_{1/2}}$. It should be mentioned that Eq. (2) assumes that repair half-life $T_{1/2}$ is much shorter than time between successive fractions of radiotherapy.

Protraction factor in (2) can be obtained from the kinetics of damage production and repair of DNA double strand breaks (DSB) [11]. In particular, the lethal damage produced by ionizing radiation and described by the term αd, corresponds to DSB caused by individual hits (or tracks). On the other hand, the term $\beta G d^2$ describes the damage caused by the interaction of DSBs produced by two tracks. Eq. (2) assumes that the interacting DSBs experience mono-exponential repair defined by repair rate μ. In the case when dose rate is constant, the double integral in (2) can be taken analytically with the following expression for G [12]:

$$G = \frac{2}{\mu T}\left[1 - \frac{1-\exp(-\mu T)}{\mu T}\right]. \tag{3}$$

It should be mentioned that although Eq. (3) relies on the assumption of constant dose rate, it serves as a good approximation for G even when R varies during irradiation of the patient [13]. In the following sections, we will incorporate Eq. (3) into a radiobiological model to evaluate the effect of dose rate in hypofractionated radiotherapy.

In the calculations of BED_{nt} and BED_{tar} described below, we consider both mono-exponential and bi-exponential repair of radiation-induced DNA damage. Unlike the former case, bi-exponential repair is characterized by two different repair channels with half-lives $T_{1/2,1}$ and $T_{1/2,2}$. The effective protraction factor for bi-exponential repair is given by the weighted sum of protraction factors for the different repair channels:

$$G = a_1 G_1 + a_2 G_2, \tag{4}$$

where a_1 and a_2 are partition coefficients, G_1 and G_2 are protraction factors defined by the repair rates $\mu_1 = \frac{\ln 2}{T_{1/2,1}}$ and $\mu_2 = \frac{\ln 2}{T_{1/2,2}}$, respectively (see Eq. (3)) [14].

To assess the effect of dose per fraction and dose rate on protraction factor, we can approximate fraction time as

$$T = T_0 + \frac{N_{MU}}{R_{MU}}, \tag{5}$$

where N_{MU} denotes number of monitor units required to deliver target dose d on a linear accelerator, R_{MU} denotes average dose rate measured in monitor units per minute and T_0 represents dose-independent component of fraction time. Note that T_0 depends on treatment parameters including number of radiation beams, treatment couch angles for each beam, positions and velocities of MLC leaves etc. When non-coplanar beams (i.e., beams characterized by different couch positions) are used for treatment, the participating therapists move the patient between successive radiation beams. In the case of multiple non-coplanar beams studied in our previous investigation [4], the associated T_0 can be significantly greater than the term $\frac{N_{MU}}{R_{MU}}$. As a result, the latter term can be neglected in Eq. (5). In contrast, $\frac{N_{MU}}{R_{MU}}$ can be the dominant contributor to fraction time in a different approach, known as Volumetric Arc Therapy (VMAT), in which a few intensity-modulated arcs (i.e., 1–4) are employed. The applicability of Eq. (5) for calculation of fraction time in VMAT is discussed in Appendix A.

To obtain a realistic estimate of $\frac{N_{MU}}{R_{MU}}$ in hypofractionated therapy with VMAT, we first notice that number of monitor units and dose per fraction are related as follows:

$$N_{MU} = \lambda d \tag{6}$$

where parameter λ depends on the utilized approach to deliver therapeutic radiation to the patient. Consider an example of VMAT with dose per fraction $d = 10$ Gy delivered with average dose rate of 400 MU/min by using co-planar arcs, one clockwise and one counter-clockwise. When intensity modulated arcs are used to irradiate deeply seated small targets (e.g., depth $>$ 5–10 cm and size $<$ 4–5 cm) it typically takes between 2 and 5 monitor units to deliver unit dose of 1 cGy $= 10^{-2}$ Gy. As a result, parameter λ varies between 2 MU/cGy and 5 MU/cGy. Consequently, delivery of 10 Gy can require between 2000 and 5000 monitor units with the corresponding time $\frac{N_{MU}}{R_{MU}}$ ranging between 5 and 12.5 min. Note that the obtained estimate for $\frac{N_{MU}}{R_{MU}}$ is greater than the typical time ($<$ 1 min) needed to dial treatment parameters on the linac console for each of the utilized volumetric arcs and start delivery of radiation to the patient.

In the current investigation, we focus on the case

$$T_0 << \min\left(\frac{N_{MU}}{R_{MU}}, T_{1/2,tar}, T_{1/2,nt}\right), \tag{7}$$

where $T_{1/2,tar}$ and $T_{1/2,nt}$ denote half-lives for malignant and normal cells, respectively. Let d_{tar} denote dose per fraction delivered to the treatment target. Under condition in (7) and assumption of mono-exponential repair in the target and OAR, protraction factors for the target (G_{tar}) and organ at risk (G_{nt}) can be obtained by substituting $\frac{\lambda d_{tar}}{R_{MU}}$ instead of T in Eq. (3):

$$G_{tar} = \frac{2R_{MU}}{\mu_{tar}\lambda d_{tar}}\left[1 - \frac{1-\exp(-\mu_{tar}\lambda d_{tar}/R_{MU})}{(\mu_{tar}\lambda d_{tar}/R_{MU})}\right] \text{ and } G_{nt} = \frac{2R_{MU}}{\mu_{nt}\lambda d_{tar}}\left[1 - \frac{1-\exp(-\mu_{nt}\lambda d_{tar}/R_{MU})}{(\mu_{nt}\lambda d_{tar}/R_{MU})}\right] \tag{8}$$

where $\mu_{tar} = \frac{\ln 2}{T_{1/2,tar}}$ and $\mu_{nt} = \frac{\ln 2}{T_{1/2,nt}}$. Eq. (8) clearly indicates that both G_{tar} and G_{nt} are non-linear functions of the ratio $\frac{d_{tar}}{R_{MU}}$.

To elucidate dependences of protraction factors G_{tar} and G_{nt} on d_{tar} and R_{MU}, these factors are plotted as functions of dose per fraction for three different dose rates: $R_{MU} = 300$, 600 and 1000 MU/min (see Fig. 1). In the calculations we used half-lives of 18 and 60 min which are typical for malignant and normal cells, respectively [15,16]. The presented results which will be important for our discussion in the subsequent sections, indicate the following: (a) G_{tar} and G_{nt} decreases with increasing d_{tar}; (b) observed changes in G_{tar} and G_{nt} with d_{tar} decrease with increasing dose rate; (c) ratio G_{tar}/G_{nt} decrease with increasing d_{tar}; (d) G_{tar}/G_{nt} increase with increasing dose rate.

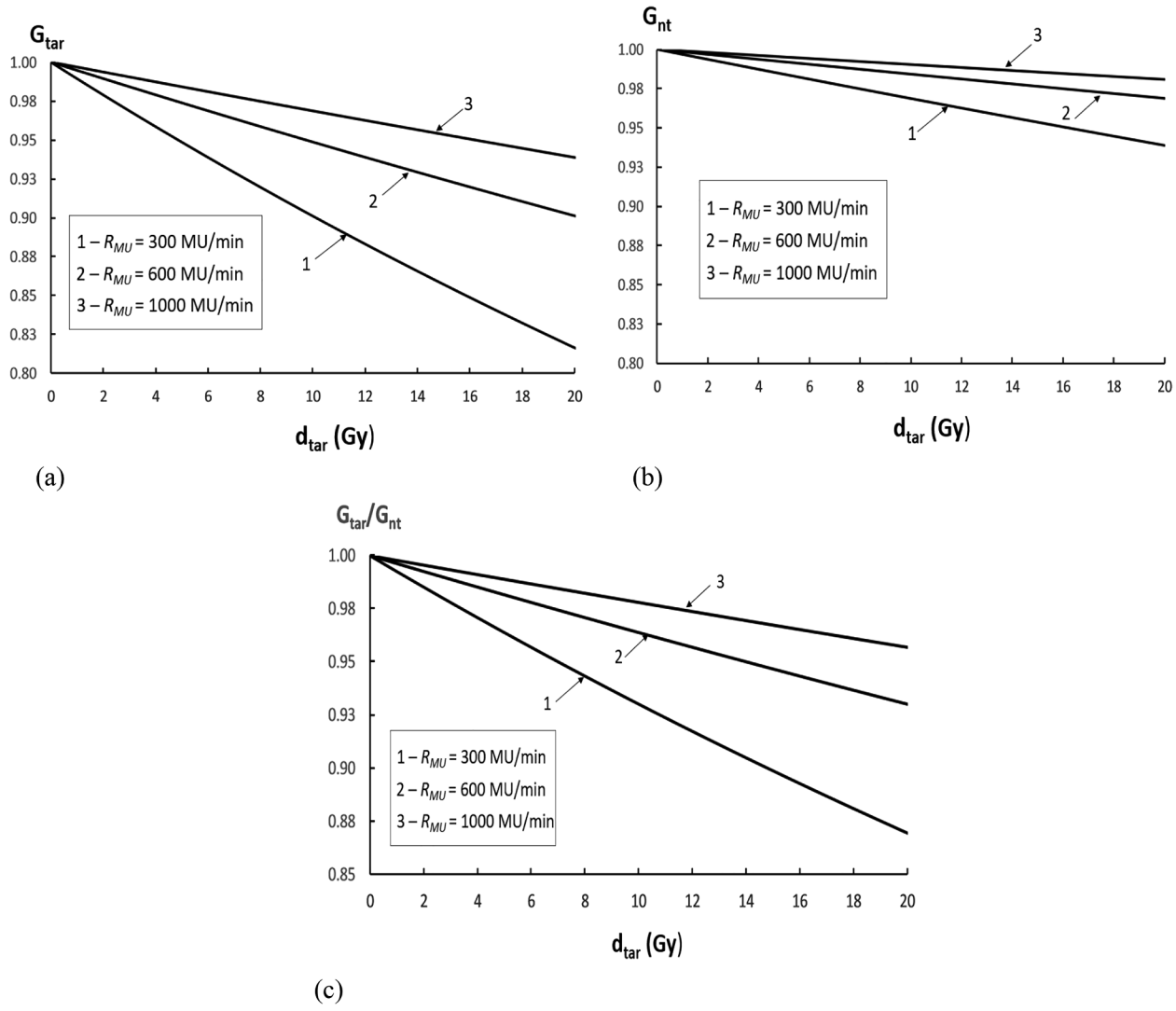

Fig. 1. Protraction factors for the target and normal tissue vs dose per fraction (see Eq. (8)): (a)$T_{1/2}$ = 18 min, (b)$T_{1/2}$ = 60 min. In the calculations we used three different values of dose rate and dose-to-MU conversion factor λ = 2.5 MU/cGy.

2.2. BED in the treatment target and organ at risk

As in the previous studies [1–3], we consider uniformly irradiated planning target volume (PTV) located in the vicinity of a critical OAR. Below we focus on the case of a serial OAR (e.g., spinal cord, chiasm). The case of a parallel OAR is described in the Appendix B.

Suppose that PTV receives dose per fraction d_{tar} while maximum dose per fraction in the OAR is $d_{nt,\max}$. The relationship between dose to the PTV and maximum dose in the OAR can be written as $d_{nt,\max} = \xi d_{tar}$, where ξ is the radiation sparing factor for the OAR. For a serial organ, the commonly used assumption is that radiobiological effect of radiation is defined by the maximum value of biologically effective dose ($BED_{nt,\max}$). The quantities BED_{tar} and $BED_{nt,\max}$ depend on the ratio of alpha and beta radio-sensitivities of malignant cells, $(\alpha/\beta)_{tar}$, and normal cells, $(\alpha/\beta)_{nt}$, number of fractions, d_{tar} and $d_{nt,\max}$. In the case when separation between PTV and OAR is sufficiently large, it is possible to achieve $\xi = \frac{d_{nt,\max}}{d_{tar}} << 1$. Conversely, in the case of when the affected OAR is in close proximity to the PTV, ξ can be close to unity. Our objective is to demonstrate that, as compared to standard fractionation, hypofractionation can either reduce or increase BED_{nt} depending on ξ, dose rate, alpha/beta ratios and repair rates in the OAR and PTV.

In the LQ model, the radiobiological effects of radiation on the target and OAR are defined by the biologically effective doses:

$$BED_{tar} = N_f d_{tar}\left(1 + \frac{G_{tar} d_{tar}}{(\alpha/\beta)_{tar}}\right) \text{ and } BED_{nt,\max} = N_f d_{nt,\max}\left(1 + \frac{G_{nt} d_{nt,\max}}{(\alpha/\beta)_{nt}}\right). \quad (9)$$

In the following derivations we consider how $BED_{nt,\max}$ varies with N_f under the assumption that BED_{tar} is fixed. As a result, we have

$$D_{tar}\left(1 + \frac{G_{tar} D_{tar}/N_f}{(\alpha/\beta)_{tar}}\right) = \text{ const.} \quad (10)$$

From Eqs. (8), (9) and (10) it follows that d_{tar} decreases with increasing number of fractions while D_{tar} increases with increasing N_f. Next, by using Eq. (9), we have

$$d_{tar}^2 = \frac{(\alpha/\beta)_{tar}}{N_f G_{tar}}(BED_{tar} - D_{tar}). \quad (11)$$

By substituting ξd_{tar} instead of $d_{nt,\max}$ into Eq. (9) and using Eq. (11), we obtain

$$BED_{nt,\max} = D_{tar}\left(\xi - \frac{\xi^2 G_{nt}}{G_{tar}\eta}\right) + \xi^2 \frac{G_{nt}}{G_{tar}\eta} BED_{tar} \quad (12)$$

where $\eta = \frac{(\alpha/\beta)_{nt}}{(\alpha/\beta)_{tar}}$. From Eq. (12) it follows that derivative $\frac{dBED_{nt,\max}}{dN_f}$ is given by

$$\frac{dBED_{nt,\max}}{dN_f} = \left(\xi - \frac{\xi^2 G_{nt}}{G_{tar}\eta}\right)\frac{dD_{tar}}{dN_f} + \frac{\xi^2}{\eta}(BED_{tar} - D_{tar})\frac{d}{dN_f}\left(\frac{G_{nt}}{G_{tar}}\right). \quad (13)$$

As mentioned previously, the current investigation focuses on the case when $T_0 << \frac{N_{MU}}{R_{MU}}$. Under the latter condition dependences of G_{nt} and G_{tar} on dose per fraction and dose rate can become important. Special cases of very low and very high dose rate, for which ratio G_{nt}/G_{tar} is independent of dose per fraction, are considered in the following section.

2.3. $BED_{nt,max}$ for very low and very high dose rates

Our objective here is to determine variations in $BED_{nt,\max}$ with number of fractions by considering special cases of very high and very low dose rates. In particular, if dose rate R_{MU} is sufficiently high so that

$$\frac{N_{MU}}{R_{MU}} = \frac{\lambda d_{tar}}{R_{MU}} << \min(T_{tar,1/2},\ T_{nt,1/2}) \quad (14)$$

then both G_{nt} and G_{tar} are approximately equal to unity (see Eq. (8)). In this case, from Eq. (13) it follows that $BED_{nt,\max}$ in the irradiated OAR increases with increasing N_f if and only if [1–3]

$$\xi < \eta. \quad (15)$$

Let us now consider another special case when R_{MU} is sufficiently small so that

$$\frac{N_{MU}}{R_{MU}} >> \max(T_{tar,1/2},\ T_{nt,1/2}). \quad (16)$$

If both target and OAR are characterized by mono-exponential repair kinetics, in the considered case we have (see Eq. (8)):

$$G_{tar} \approx \frac{2R_{MU}}{\mu_{tar}\lambda d_{tar}} \text{ and } G_{nt} \approx \frac{2R_{MU}}{\mu_{nt}\lambda d_{tar}}. \quad (17)$$

From Eq. (17) it follows that $G_{nt}/G_{tar} \approx \frac{\mu_{tar}}{\mu_{nt}}$. By using Eq. (13), we conclude that when radiation is delivered with a very low dose rate, $BED_{nt,\max}$ increases with increasing N_f if and only if

$$\xi < \frac{\mu_{nt}}{\mu_{tar}}\eta. \quad (18)$$

To elucidate the dependence of $BED_{nt,\max}$ on dose rate, let us assume that the following two conditions are fulfilled: $\frac{\mu_{nt}}{\mu_{tar}} < 1$ and $\frac{\mu_{nt}}{\mu_{tar}}\eta < \xi < \eta$. Because under these assumptions condition in (15) is satisfied, in the case of high dose rate $BED_{nt,\max}$ increases with increasing number of fractions.

Consequently, hypofractionation lowers $BED_{nt,\max}$ as compared to standard fractionation. Conversely, under the same assumptions, condition in (18) is not satisfied. As a result, hypofractionation increases $BED_{nt,\max}$ relative to standard fractionation and/or hyperfractionation in the case of very low dose rate.

The obtained result can be stated as follows: for the same dose distribution characterized by OAR sparing factor ξ, hypofractionation can either decrease or increase $BED_{nt,\max}$ depending on dose rate. In Section 3 this conclusion will be confirmed by considering several examples with dose rates typically used in radiotherapy with external beams.

2.4. $BED_{nt,max}$ in the case of arbitrary dose rate

Although analytical dependence of $BED_{nt,\max}$ on the number of fractions for different dose rates is not known, we are able to qualitatively assess this dependence as follows. Let us assume that for a standard dose per fraction of 2 Gy and considered dose rate, the ratio $\frac{N_{MU}}{R_{MU}}$ is sufficiently small so that G_{nt} and G_{tar} are approximately unity. Suppose first that condition in Eq. (15) is satisfied. As a result, $BED_{nt,\max}$ initially decreases with decreasing number of fractions. To maintain fixed BED_{tar}, dose per fraction increases with decreasing N_f. Consequently, both G_{nt} and G_{tar} decrease as number of fractions decreases (see Fig. 1). The ratio G_{tar}/G_{nt} varies with number of fractions (except in the unlikely case $\mu_{nt} = \mu_{tar}$). Note that for a number of analyzed tumor cell lines in vitro, the geometric average of $T_{1/2}$ is less than 17 min [10]. Conversely, for normal tissues, reported values of $T_{1/2}$ are significantly higher (e.g., 70.2 min [16]). The shorter $T_{1/2}$ in the target results in a faster reduction in G_{tar} with increased dose per fraction relative to the observed reduction in G_{nt} (see Fig. 1). Consequently, the ratio G_{tar}/G_{nt} decreases with decreasing number of fractions. Suppose that for some number of fractions $\widetilde{N}_f$ the ratio G_{tar}/G_{nt} becomes small enough so that $\xi > \frac{G_{tar}}{G_{nt}}\eta$ and the first term (i.e., $(\xi - \frac{\xi^2 G_{nt}}{G_{tar}\eta})\frac{dD_{tar}}{dN_f}$) in Eq. (13) becomes negative. Because derivative $\frac{d}{dN_f}\left(\frac{G_{nt}}{G_{tar}}\right)$ is negative while the difference $BED_{tar} - D_{tar}$ is positive (see Eq. (11)), the second term $\frac{\xi^2}{\eta}(BED_{tar} - D_{tar})\frac{d}{dN_f}\left(\frac{G_{nt}}{G_{tar}}\right)$ in Eq. (13) is also negative. As a result, further lowering the number of fractions causes an increase in $BED_{nt,\max}$. In other words, for dose rates used in clinical practice, we expect to observe cases for which decreasing number of fractions can initially lower biologically effective dose in the OAR; however, as N_f continues to decrease, $BED_{nt,\max}$ will eventually increase (see examples in Section 3).

Second, let us now consider the case when condition in Eq. (15) is not satisfied. As shown previously [1–3], in this case decreasing number of fractions leads to an increased BED_{nt} when the effect of dose rate is neglected. How does this increase in BED_{nt} depend on dose rate? To answer this question, let us begin with the case of sufficiently high dose rate so that G_{tar}/G_{nt} is approximately unity. As a result, variations in BED_{nt} caused by varying N_f are defined by the first term in Eq. (13). Since D_{tar} increases with N_f, the first term in the expression for $\frac{dBED_{nt,\max}}{dN_f}$ in Eq. (13) is negative. Consider the case $\mu_{tar} > \mu_{nt}$ for which $\frac{G_{nt}}{G_{tar}} > 1$. Suppose that dose rate is lowered and, as a result, $\frac{G_{nt}}{G_{tar}}$ is increased. As a result, the first term in Eq. (13) increases in magnitude. Consequently, lowering dose rate makes $BED_{nt,\max}$ increase faster with decreasing N_f as compared to the case of very high dose rate. This conclusion will be illustrated by considering examples in Section 3 (see Fig. 2 and Table 1).

2.5. Calculation of BED_{nt} for different treatment plans

2.5.1. Plan parameters

To study the effect of dose rate on BED_{nt}, we considered three treatment plans. Each plan utilized three VMAT arcs with 6 MV photons, different start and stop gantry angles. All plans were created in Eclipse treatment planning system (v. 11, Varian Medical Systems, Palo Alto, CA, USA). The mean target dose to the PTV, number of fractions and dose per fraction for each plan were 70 Gy, 35 and 2 Gy, respectively. The maximum cord dose for the first, second and third plans were 16.8, 20.3 and 28 Gy, respectively.

2.5.2. Radiobiological parameters

Spinal cord is thought of as a serial structure [17]. In the performed calculations, bi-exponential repair of sublethal damage with half-lives of 42 and 228 min was assumed for the cord [15,18]. Note also that in the calculations of $BED_{nt,\max}$ we used equal fractions of repair through the fast and slow channels (i.e., $a_1 = a_2 = 0.5$ in Eq. (4)) and $\alpha/\beta = 3$ Gy. In contrast, for malignant cells we used $\alpha/\beta = 10$ Gy and the assumption of mono-exponential repair. The considered half-lives for malignant cells were $T_{1/2,tar}$=5, 18 and 30 min [10,15].

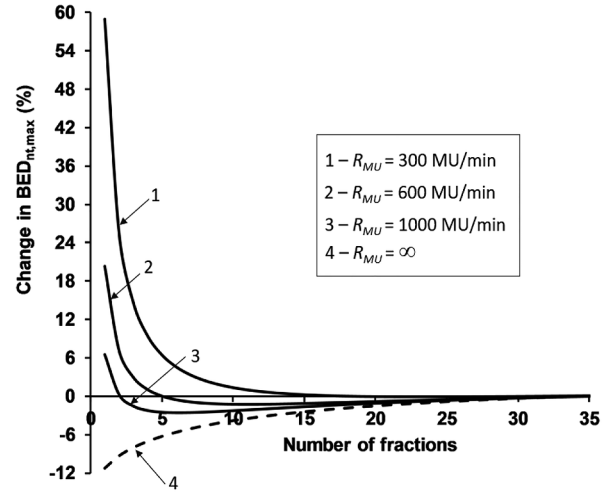

(a) - $T_{1/2,tar} = 5$ min, $\xi = 0.24$

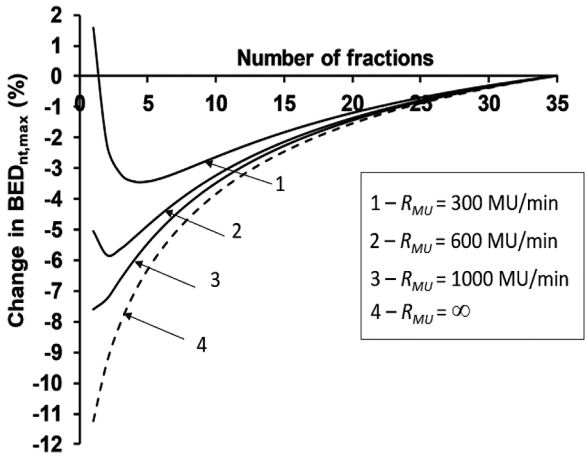

(b) - $T_{1/2,tar} = 18$ min, $\xi = 0.24$

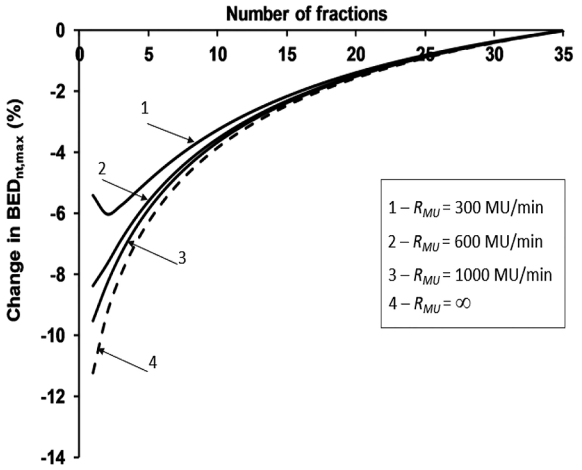

(c) - $T_{1/2,tar} = 30$ min, $\xi = 0.24$

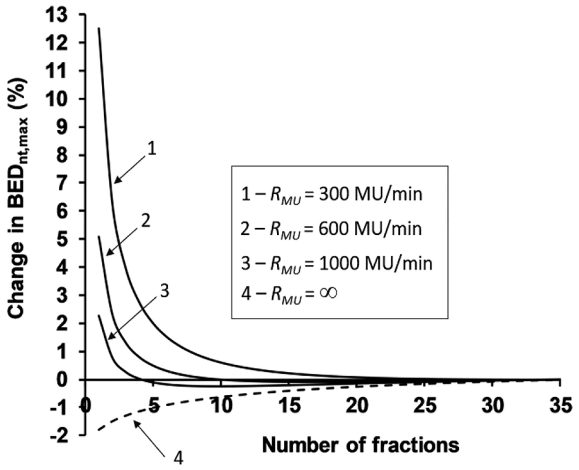

(d) - $T_{1/2,tar} = 18$ min, $\xi = 0.29$

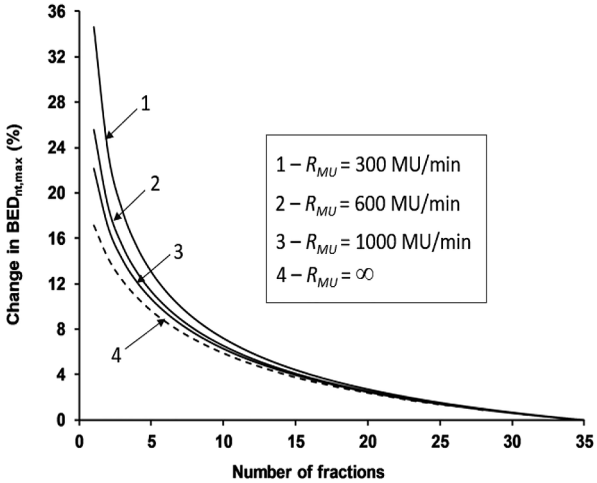

(e) - $T_{1/2,tar} = 18$ min, $\xi = 0.40$

Fig. 2. Change in $BED_{nt,\max}$ as a function of number of fractions. The results were obtained for $T_{1/2,tar}$ = 5, 18 and 30 min and three different values of sparing factor: ξ = 0.24, 0.29 and 0.40. For spinal cord, bi-exponential repair of sublethal damage with half-times of 42 and 228 min was assumed. In the calculations three different dose rates were used R_{MU} = 300 , 600 and 1000 MU/min. Dashed lines in Fig. 2a–e describe the case of an infinitely high dose rate for which the corresponding fraction time is zero.

Table 1
Maximum EQD_{2Gy} in the spinal cord for several different dose rates and number of fractions under the condition of fixed EQD_{2Gy} = 70 Gy in the target.

Dose rate (MU/min)	Sparing factor ξ	Number of fractions					
		3	4	5	10	20	35
		EQD_{2Gy} (Gy)					
300	0.4	30.2	28.0	26.7	23.8	22.1	21.3
	0.5	43.9	40.3	38.0	32.9	29.7	28.0
600	0.4	26.9	25.8	25.0	23.2	21.9	21.3
	0.5	39.1	37.0	35.6	32.0	29.5	28.0
1400	0.4	25.2	24.5	24.0	22.8	21.9	21.3
	0.5	36.4	35.1	34.2	31.5	29.4	28.0
2400	0.4	24.6	24.1	23.7	22.7	21.8	21.3
	0.5	35.6	34.5	33.7	31.4	29.3	28.0

2.5.3. Procedure for calculation of $BED_{nt,max}$

In order to determine target dose D_{tar} as a function of N_f for each plan, we used Eq. (10). Subsequently, we used Eq. (12) to calculate $BED_{nt,\max}$. In the calculations we also used Lea and Catcheside formula for protraction factor G (see Eqs. (3) and (8)). The applicability of Eq. (3) was verified by evaluating the previously measured protraction factors [19].

2.6. Equivalent total dose in 2-Gy fraction (EQD_{2Gy})

In addition to *BED*, we also determined EQD_{2Gy} for the cord (see next section). By definition, EQD_{2Gy} is the total dose delivered in 2-Gy fractions that would give the same log cell kill as the considered treatment regimen [7]. The relationship between *BED* and EQD_{2Gy} is given by

$$EQD_{2Gy} = \frac{BED}{1 + \frac{2\ Gy}{(\alpha/\beta)}}. \tag{19}$$

For spinal cord with the assumed alpha/beta ratio of 3 Gy, the maximum EQD_{2Gy} is obtained by dividing $BED_{nt,\max}$ by 1 + 2/3 = 1.67.

3. Results

In this section we report changes in $BED_{nt,\max}$ in the spinal cord caused by varying number of fractions. Note that calculations of $BED_{nt,\max}$ were performed under the condition of fixed biologically effective dose in the target. All results were obtained by using fixed value of cGy-to-MU conversion factor $\lambda = 2.5$ MU/cGy.

The data in Fig. 2 demonstrate the calculated changes in $BED_{nt,\max}$ caused by varying number of fractions by using standard fractionation as the baseline. In the calculations we used dose rates of 300, 600 and 1000 MU/min and three different values of sparing factor: $\xi = 0.24$, $\xi = 0.29$ and $\xi = 0.40$. The corresponding maximum doses to the cord for the standard fractionation were 16.8, 20.3 and 28 Gy, respectively. Note that dashed lines in Fig. 2a–e represent changes in $BED_{nt,\max}$ calculated by setting treatment time to zero (i.e., under the assumption of infinitely high dose rate for which the effect of radiation protraction can be neglected).

Table 1 contains maximum EQD_{2Gy} in the spinal cord. The calculations were performed for different dose rates and number of fractions, $\xi = 0.4$ and 0.5, and $T_{1/2,tar}$=5 min. Like in Fig. 2, the results in Table 1 were obtained by assuming bi-exponential decay for the cord with half-lives of 42 and 228 min.

4. Discussion

4.1. Radiobiological model

In the current study, the effect of dose rate on BED_{nt} is considered by varying the number of fractions under the condition of fixed biologically effective dose in the treatment target. The main result of our investigation can be summarized as follows: depending on the dose rate, hypofractionation can either decrease or increase BED_{nt} as compared to standard fractionation and/or hyperfractionation. It should be realized that for a standard dose per fraction d = 2 Gy and commonly utilized dose rate varying between 300 and 1000 MU/min, the component of fraction time which is dependent on dose rate is smaller than typical repair half-life (i.e., $T_{1/2} > 5$–10 min). As a result, the effect of dose rate on radiobiological properties of hypofractionation generally becomes significant for larger values of dose per fraction (i.e., $d > 5$–10 Gy).

As mentioned earlier, the current study is based on the linear-quadratic model for cell kill. Several recent studies claimed that this model needed to be modified or replaced for $d > 5$–10 Gy [20,21]. Conversely, these claims were disputed in [22,23]. Consequently, caution should be employed when the LQ model is applied for *BED* calculations for these values of dose per fraction. Also, it should be kept in mind that while the current study focuses on the effect of dose rate on radiobiological properties of hypofractionated regimens, other important factors including tumor hypoxia, reoxygenation and repopulation of malignant cells [24] have been shown to affect treatment outcome. Investigation of these additional factors is beyond the scope of the current work.

It should be realized that the obtained results are based on the assumption of exponential repair of sublethal damage caused by radiation. A different radiobiological model with “reciprocal repair” was suggested by Fowler and co-authors [26,27]. The latter model was shown to reproduce many of the features of repair kinetics previously modeled by using assumption of multi-exponential repair. Reciprocal repair has significant clinical implications due to the fact that the apparent repair rate is dependent on dose [27]. The effect of reciprocal repair on *BED* in hypofractionated regimens will be evaluated in our future studies.

4.1.1. Effect of dose rate on BED_{nt}

Previous studies [1–3] reported a threshold value of radiation sparing factor $\xi_{th} = \eta$ below which hypofractionation can lower BED_{nt} as compared to standard fractionation. It is important to mention that in these studies the effect of radiation protraction was neglected. In another investigation [4], it was shown that this effect modifies the threshold value of radiation sparing factor; i.e., under the condition that fraction time is independent of dose per fraction $\xi_{th} = \frac{G_{tar}}{G_{nt}}\eta$. Note that in the previously developed radiobiological model [1–4], BED_{nt} monotonically increases with number of fractions when $\xi < \xi_{th}$. In the opposite case $\xi > \xi_{th}$, BED_{nt} monotonically decreases with increasing N_f.

In contrast, in the considered model repair of radiation induced sublethal damage takes place during fraction time which depends on the ratio of dose per fraction and dose rate. The obtained results clearly indicate that BED_{nt} is dependent on dose rate (see Fig. 2). In particular, in the case of relatively low dose rate (e.g., R_{MU} = 300 MU/min), BED_{nt} can initially decrease with decreasing N_f, reach its minimum at certain $N_f = \widetilde{N}_f$ and eventually start to increase upon further reduction in N_f (see Fig. 2a–c). To conclude, under certain conditions there can exist an optimum number of fractions $\widetilde{N}_f > 1$ which provides the smallest achievable BED_{nt} for a given dose rate.

It should be mentioned that the obtained results are based on the assumption that treatment time is proportional to dose per fraction and inversely proportional to the utilized dose rate. It is known that during delivery of VMAT treatments, dose rate can vary with angle of rotation. To elucidate the effect of variable dose rate on *BED*, a number of

different SBRT plans were delivered on a Trilogy linac by using different number of monitor units for the same plan (see Appendix A). The obtained results clearly indicate that the determined average dose rate is lower than the nominal dose rate; however, variations in dose rate cause relatively small changes (i.e., $\leqslant 1\%$) in BED_{nt} and BED_{tar}.

4.1.2. Dependence of BED_{nt} on $\frac{T_{1/2,tar}}{T_{1/2,nt}}$

By examining the expression for protraction factor G in Eq. (3), it is easy to see that the effect of protraction increases with increasing fraction time T. Increasing dose rate causes a reduction in fraction time with the corresponding increase in G. As discussed previously, under the assumption that malignant cells repair radiation induced damage generally faster than normal cells, increasing dose rate corresponds to increased ratio $\frac{G_{tar}}{G_{nt}}$ for the same target dose (see Fig. 1c). In turn, increased ratio $\frac{G_{tar}}{G_{nt}}$ makes it easier to satisfy condition in (14) and, as a result, easier to achieve reduction in BED_{nt} for hypofractionated regimens as compared to standard fractionation. The dependences of BED_{nt} on number of fractions in Fig. 2 confirm this conclusion. Specifically, in the case of short $T_{1/2,tar} = 5$ min, $\xi = 0.24$ and zero fraction time (see dashed line in Fig. 2a), BED_{nt} in the cord decreased by approximately 11% when number of fractions was reduced from 35 to 1. Conversely, when the effect of non-zero fraction time was assessed for dose rate of 300 MU/min, varying number of fractions from 35 to 1 resulted in an approximately 60% increase in BED_{nt} instead of the 11% reduction. When the dose rate was increased to 1000 MU/min, we observed maximum increase of only 6% in BED_{nt} for a single fraction treatment.

In the case of a longer $T_{1/2,tar} = 18$ min, $\xi = 0.24$ and dose rate of 300 MU/min, maximum increase in BED_{nt} was about 2% for a single fraction treatment (see Fig. 2b). It is interesting that in the latter case maximum reduction in BED_{nt} was 3.5% and was observed for $N_f = 4$ and 5. For even longer $T_{1/2,tar} = 30$ min, the effect of radiation protraction was small enough so that for all considered dose rates we observed a decrease in BED_{nt} with decreasing N_f from its baseline value $N_f = 35$. The decrease in BED_{nt} was monotonic except in the case of the lowest considered dose rate of 300 MU/min. In the latter case, minimum of BED_{nt} was reached at $N_f = 2$.

For radiation sparing factor $\xi = 0.29$, just below the threshold value $\xi_{th} = 0.3$, setting fraction time to zero and varying N_f from 35 to unity resulted in BED_{nt} decreasing by 2%. In contrast, for dose rate 300 MU/min, a 12.5% increase in BED_{nt} was observed (Fig. 2d). In the case $\xi = 0.40$, biologically effective dose in the cord increased with decreasing number of fractions for all considered dose rates, with the maximum increase in BED_{nt} varying between approximately 35% and 22% for dose rates of 300 MU/min and 1000 MU/min, respectively (Fig. 2e).

For certain tumor cell lines, in-vitro studies demonstrated very long repair half-lives (e.g., > 5 h for human leukemic cells [10]). In contrast, much shorter repair times (e.g., 0.5 h [25]) were reported for rectal tissue based on the analysis of complications due to brachytherapy treatments. Since fraction time is inversely proportional to dose rate, decreasing dose rate in the case $T_{1/2,nt} < T_{1/2,tar}$ leads to increased ratio $\frac{G_{tar}}{G_{nt}}$ which makes it easier to lower BED_{nt} by decreasing number of fractions (see Eq. (14)). The performed numerical calculations (not shown here for brevity) confirm that under the condition $T_{1/2,nt} < T_{1/2,tar}$, lower values of BED_{nt} can be achieved by decreasing dose rate; however, variations in BED_{nt} with dose rate are expected to be small because in the considered case, fraction times are typically shorter than both $T_{1/2,nt}$ and $T_{1/2,tar}$.

4.1.3. Potential clinical ramifications

The results of this study indicate that the effect of finite dose rate on biologically effective dose in hypofractionated regimens can be significant (i.e., > 5% variation in BED_{nt}). Although reliable data on repair rates *in vivo* for different malignant and normal cells are currently lacking, by using published values of $T_{1/2,nt}$ and $T_{1/2,tar}$, we have shown that while in the case of low dose rate hypofractionation can lead to a significantly increased BED_{nt}, a significantly smaller increase or even a decrease in BED_{nt} can be achieved for higher dose rates. As a result, in order to realize radiobiological advantages of hypofractionated regimens as compared to standard fractionation, it appears advantageous to deliver hypofractionated treatments with the highest dose rate available. For conventional clinical linear accelerators with flattening filter, utilized dose rate normally ranges between 300 and 1000 MU/min. Flattening filter free (FFF) units are capable of significantly higher dose rates (e.g., 1400 and 2400 MU/min). The obtained results (see Table 1) clearly indicate that the use of high dose rate on FFF linacs can be advantageous in the case of SBRT and short $T_{1/2,tar}$ (i.e., < 5–10 min) observed for several tumor cell lines [10].

Note also in the case of malignant cells with short repair half-life $T_{1/2,tar} < T_{1/2,nt}$, maximum increase in BED_{nt} was observed for $N_f = 1$ (e.g., see Fig. 2a). Consequently, the obtained results indicate that fractionated SBRT and SRS (e.g., $N_f = 5$) can be radiobiological advantageous compared to single-fraction treatments.

5. Conclusions

The obtained results indicate that for the same dose distribution, hypofractionation can either reduce or increase BED_{nt} in the affected organ at risk as compared to standard fractionation and/or hyperfractionation depending on the utilized dose rate and ratio of repair half-lives $\frac{T_{1/2,tar}}{T_{1/2,nt}}$. The considered cases also demonstrate that BED_{nt} can vary with number of fractions in a non-monotonic fashion; i.e., BED_{nt} can initially decrease with decreasing N_f, reach its minimum at certain $N_f = \tilde{N}_f > 1$ and start to increase upon further reduction in N_f. Note that $\tilde{N}_f$ represents the optimum number of fractions (for a given BED_{tar}) which corresponds to the minimum BED_{nt}.

The results of this study clearly indicate that in addition to the OAR sparing factor ξ and α/β ratio for malignant and normal cells, radiobiological comparison of hypofractionation and standard fractionation should also take into account repair rates in the target and OAR as well as dose rate.

Declaration of Competing Interest

The authors declare that they have no known competing financial interests or personal relationships that could have appeared to influence the work reported in this paper..

Appendix A

Eq. (5) assumes that fraction time scales linearly with dose per fraction. To verify this assumption, treatment plans for four previously treated SBRT cases were considered. In every case, a VMAT plan with dose per fraction of 10 Gy and five fractions was originally created in Eclipse treatment planning system (v. 11, Varian Medical Systems, Palo Alto, CA, USA) by using two co-planar arcs. Subsequently, four more additional plans with fraction doses of 5, 15, 20 and 25 Gy were produced by changing only one parameter: dose per fraction. The plans were examined to confirm that relative dose distribution (i.e., normalized to the maximum dose) was the same for all five plans. Subsequently, each plan was delivered on a Varian Trilogy with nominal rate of 600 MU/min. Delivery time for every plan was measured with a stopwatch. It was found that the dose-independent component of fraction time T_0 in Eq. (5) was less than 0.5 min. Note that T_0 was neglected in the calculations of protraction factors and biologically effective doses listed in Table 2.

Table 2
Monitor units, delivery times, protraction factors and BEDs for different doses per fraction and $T_{1/2} = 5$ min.

Case	d	N_{MU}		T_m	T_p	G_m	G_p	$G_p - G_m$	$BED_{tar,p} - BED_{tar,m}$	$BED_{nt,p} - BED_{nt,m}$
N#	(Gy)	Arc 1	Arc 2	(min)	(min)			diff(%)	diff(%)	diff(%)
1	5	770	771	2.75	2.57	0.884	0.891	0.8	0.2	0.5
1	10	1540	1543	5.39	5.14	0.791	0.799	1.0	0.5	0.8
1	15	2310	2314	8.03	7.71	0.713	0.722	1.3	0.6	1.0
1	20	3081	3086	10.67	10.28	0.646	0.655	1.4	0.8	1.1
1	25	3851	3857	13.03	12.85	0.595	0.599	0.6	0.4	0.5
2	5	638	684	2.57	2.20	0.891	0.906	1.6	0.5	1.0
2	10	1276	1367	4.70	4.41	0.814	0.824	1.2	0.6	0.9
2	15	1914	2052	6.86	6.61	0.746	0.753	1.0	0.5	0.8
2	20	2552	2734	9.05	8.81	0.686	0.692	0.9	0.5	0.7
2	25	3190	3418	11.28	11.01	0.632	0.638	1.0	0.6	0.8
3	5	1118	1188	4.05	3.84	0.836	0.844	0.9	0.3	0.5
3	10	2236	2377	8.00	7.69	0.714	0.722	1.2	0.5	0.8
3	15	3354	3565	11.81	11.53	0.621	0.627	1.0	0.5	0.7
3	20	4472	4753	15.73	15.38	0.544	0.550	1.1	0.6	0.9
3	25	5590	5942	19.49	19.22	0.485	0.489	0.8	0.4	0.6
4	5	1045	1045	3.58	3.48	0.853	0.857	0.4	0.1	0.3
4	10	2090	2089	7.22	6.97	0.736	0.743	1.0	0.4	0.7
4	15	3135	3134	10.61	10.45	0.648	0.651	0.6	0.3	0.4
4	20	4181	4178	14.13	13.93	0.573	0.577	0.7	0.4	0.5
4	25	5226	5223	17.66	17.42	0.512	0.516	0.8	0.4	0.6

Dosimetric parameters for the considered plans are listed in Table 2. During delivery of volumetric arcs, both dose rate and angular velocity of the rotating gantry vary. According to our observation, the actual dose rate was lower than the nominal dose rate. As a result, measured fraction time (T_m) exceeded predicted fraction time $\left(T_p = \frac{N_{MU}}{R_{MU}}\right)$ in each case. To verify applicability of Eq. (5), protraction factors G_m and G_p were calculated by using T_m and T_p, respectively. Note that in the case $T_{1/2} = 5$ min, the relative difference $100\cdot\left(\frac{G_p}{G_m} - 1\right)$ was within 1.6%. In addition to protraction factors, Table 2 also includes changes in biologically effective doses in the target and OAR due to the difference between T_m and T_p. Let $BED_{tar,m}$ and $BED_{tar,p}$ denote biologically effective doses in the target calculated by using alpha/beta ratio of 10 Gy and protraction factors G_m and G_p, respectively. Likewise, let $BED_{nt,m}$ and $BED_{nt,p}$ denote biologically effective doses in the OAR determined for alpha/beta ratio of 3 Gy and protraction factors G_m and G_p, respectively. According to the data from Table 2, the relative difference $100\cdot\left(\frac{BED_{tar,p}}{BED_{tar,m}} - 1\right)$ for the target was within 0.8% while the relative difference $100\cdot\left(\frac{BED_{nt,p}}{BED_{nt,m}} - 1\right)$ for the organ at risk was within 1.1%.

It should be mentioned that fraction time in hypofractionated treatments can exceed or be comparable to repair half-lives for the target and normal tissue. For example, for fraction dose of 10 Gy, the measured fraction time varied from 5.1 min to 7.7 min (see Table 2). For fraction dose of 25 Gy, the longest fraction time was approximately 19 min. Note that in the calculations of *BED* and protraction factors listed in Table 2, a short repair time of 5 min was used for both malignant and normal cells. For longer repair times (e.g., $T_{1/2,tar} = 18$ min [10] and $T_{1/2,nt} = 30$ min [25]), the difference between protraction factors G_m and G_p was within 0.5%. The corresponding differences between *BED*s in the target and/or OAR were within 0.4%.

In summary, the obtained results indicate that differences between measured fraction times and those predicted by using equation (5), result in relatively small differences in protractions factors and biologically effective doses.

Appendix B

In contrast to a serial OAR, the radiobiological effect of radiation for a parallel OAR is better described by the average BED_{nt} [3]. In order to determine this quantity, it is convenient to divide the considered QAR into N_V voxels. Each voxel is considered small enough so that variations of the absorbed dose in a voxel can be neglected. Let $BED_{nt,j}$ denote biologically effective dose in the jth voxel. The average BED_{nt} is defined as

$$\langle BED_{nt}\rangle \equiv \frac{1}{N_V}\sum_{j=1}^{N_V} BED_{nt,j}. \tag{B.1}$$

In the derivations below, dose distribution in the OAR will be characterized by two parameters:

$$\langle\xi\rangle = \frac{1}{N_V}\sum_{j=1}^{N_V}(d_{nt,j}/d_{tar}) \text{ and } \langle\xi^2\rangle = \frac{1}{N_V}\sum_{j=1}^{N_V}(d_{nt,j}/d_{tar})^2. \tag{B.2}$$

where $d_{nt,j}$ denotes absorbed dose in the jth voxel.

By using (B.1) and (B.2), we obtain (see Eq. (12))

$$\langle BED_{nt}\rangle = D_{tar}\left(\langle\xi\rangle - \frac{<\xi^2> G_{nt}}{G_{tar}\eta}\right) + \langle\xi^2\rangle\frac{G_{nt}}{G_{tar}\eta}BED_{tar}. \tag{B.3}$$

Note that Eq. (B.3) follows from Eq. (12) if we replace ξ with $\langle\xi\rangle$ and replace ξ^2 with $\langle\xi^2\rangle$. By using the same argument as in Section 2, it is straightforward to show that under conditions $\frac{\mu_{nt}}{\mu_{tar}} < 1$ and $\frac{\mu_{nt}}{\mu_{tar}}\eta < \frac{<\xi^2>}{<\xi>} < \eta$, hypofractionation lowers $<BED_{nt}>$ when dose rate is sufficiently high so that both G_{nt} and G_{tar} are close to unity. Conversely, under the same conditions and sufficiently low dose rate so that inequality in Eq. (17) is satisfied,

hypofractionation increases $<BED_{nt}>$.

Funding

This research did not receive any support from funding agencies in the public, commercial, or not-for-profit sectors.

References

[1] Mizuta M, Takao S, Date H, et al. A mathematical study to select fractionation regimen based on physical dose distribution and the linear-quadratic model. Int J Rad Oncol Biol Phys 2012;84:829–33.
[2] Gay HA, Jin JY, Chang AJ, Ten Haken RK. Utility of normal tissue-to-tumor a/b ratio when evaluating isodoses of isoeffective radiation therapy treatment plans. Int J Rad Oncol Biol Phys 2013;85:e81–7.
[3] Unkelbach J, Craft D, Salari E, Ramakrishnan J, Bortfeld T. The dependence of optimal fractionation schemes on the spatial dose distribution. Phys Med Biol 2013;58:159–67.
[4] Kuperman VY. Effect of radiation protraction in hypofractionated radiotherapy. Med Phys 2018;45:3442–8.
[5] Myerson RJ. Normal tissue dose conformality measures to guide radiotherapy fractionation decisions. Med Phys 2011;38:1799–805.
[6] Barendsen GW. Dose fractionation, dose rate and iso-effect relationships for normal tissue responses. Int J Rad Oncol Biol Phys 1982;8:1981–97.
[7] Fowler JF. 21 years of biologically effective dose. Br J Radiol 2010;83:554–68.
[8] Thames HD. An 'Incomplete-repair' model for survival after fractionated and continuous irradiations. Int J Rad Biol 1985;47:319–39.
[9] Dale RG. The application of the linear-quadratic dose-effect equation to fractionated and protracted radiotherapy. Br J Radiol 1985;58:515–28.
[10] Brenner DJ, Hall EJ. Conditions for the equivalence of continuous and pulsed low dose rate brachytherapy. Int J Rad Oncol Biol Phys 1991;20:181–90.
[11] Sachs RK, Hahnfeld P, Brenner DJ. The link between low-LET dose-response relations and the underlying kinetics of damage production/repair/misrepair. Int J Radiat Biol 1997;72(4):351–74.
[12] Lea DE, Catcheside DG. The mechanism of the induction by radiation of chromosome aberrations in tradescantia. J Genet 1942;44:216–45.
[13] Kuperman VY, Spradlin GS. Use of radiation protraction to escalate biologically effective dose to the treatment target. Med Phys 2011;38:6553–660.
[14] Kuperman VY, Spradlin GS. Effect of variable dose rate on biologically effective dose. Int J Rad Biol 2013;89:889–97.
[15] Fowler JF, Welsh JS, Howard SP. Loss of biological effect in prolonged fraction delivery. Int J Rad Oncol Biol Phys 2004;59:242–9.
[16] Brenner DJ, Armour E, Corry P, Hall EJ. Sublethal damage repair times for a late-responding tissue relevant to brachytherapy (and external-beam radiotherapy): implications for new brachytherapy protocols. Int J Rad Oncol Biol Phys 1998;41:135–8.
[17] Bentzen SM, Harari PM, Mehta MP, Tomé WA. Radiation Oncology Advances. Springer Science and Business Media, LLC; 2008.
[18] Ang KK, Jiang GL, Guttenberger R, et al. Impact of spinal cord repair kinetics on the practice of altered fractionation schedules. Radiother Oncol 1992;25:287–94.
[19] Kuperman VY, Ventura AM, Sommerfeldt M. Effect of radiation protraction in intensity-modulated radiation therapy with direct aperture optimization: a phantom study. Phys Med Biol 2008;53:3279–92.
[20] Guerrero M, Li XA. Extending the linear–quadratic model for large fraction doses pertinent to stereotactic radiotherapy. Phys Med Biol 2004;49:4825–35.
[21] Kirkpatrick JP, Meyer JJ, Marks LB. The L-Q model is inappropriate to model high-dose per fraction effects. Semin Radiat Oncol 2008;18:240–3.
[22] Brenner DJ. The linear-quadratic model is an appropriate methodology for determining isoeffective doses at large doses per fraction. Semin Radiat Oncol 2008;18:234–9.
[23] Shuryak I, Carlson DJ, Brown JM, Brenner DJ. High-dose and fractionation effects in stereotactic radiation therapy: analysis of tumor control data from 2965 patients. Radiother Oncol 2015;115:327–34.
[24] Carlson DJ, Keall PJ, Loo BW, Chen ZJ, Brown JM. Hypofractionation results in reduced tumor cell kill compared to conventional fractionation for tumors with regions of hypoxia. Int J Radiat Oncol Biol Phys 2011;79(4):1188–95.
[25] Roberts SA, Hendry JH, Swindell R, Wilkinson JM, Hunter RD. Compensation for changes in dose-rate in radical low-dose-rate brachytherapy: a radiobiological analysis of a randomised clinical trial. Radiother Oncol 2004;70(1):63–74.
[26] Fowler JF. Is repair of DNA strand break damage from ionizing radiation second-order rather than first-order? A simpler explanation of apparently multiexponential repair. Radiat Res 1999;152:124–36.
[27] Dale RG, Fowler JF, Jones B. A new incomplete-repair model based on a 'reciprocal-time' pattern of sublethal damage repair. Acta Oncol 1999;38:919–29.